Toxicology Research

PAPER

Cite this: *Toxicol. Res.*, 2015, **4**, 1498

Toxicity evaluation and translocation of carboxyl functionalized graphene in *Caenorhabditis elegans*†

Junnian Yang,‡[a,b] Yunli Zhao,‡[a] Yanwen Wang,[c] Haifang Wang[c] and Dayong Wang*[a]

Carboxyl functionalized graphene (G-COOH) can be potentially used for biosensing and medical applications. However, little is known about the *in vivo* behavior and toxicity of G-COOH. To investigate the *in vivo* translocation and toxicity of G-COOH and the underlying cellular mechanism, we employed *Caenorhabditis elegans* as a model for toxicological study. Prolonged exposure to 0.01–100 mg L^{-1} of G-COOH from L1-larvae to adult day-1 did not cause any adverse effects on the lifespan, development, or functions of the intestine, neurons, and reproductive organs in exposed nematodes and their progeny. After prolonged exposure, G-COOH was not translocated into the secondary targeted organs such as reproductive organs and neurons or the body of the progeny of exposed nematodes. In the intestinal cells, G-COOH was mainly deposited in small-vesicle structures such as peroxisomes and lysosomes adjacent to microvilli and moderately deposited in the cytosol. Meanwhile, G-COOH exposed nematodes showed normal development and function of the intestine and normal biological function of the intestinal barrier. Moreover, G-COOH exposed nematodes had normal defection behavior and developmental state of AVL and DVB neurons that control the defecation behavior. Therefore, the G-COOH translocation pattern and functional state of the intestinal barrier and/or the defecation state may contribute greatly to the *in vivo* behavior and toxicity of G-COOH at concentrations less than 100 mg L^{-1} in nematodes. Our results provide useful information on the *in vivo* properties of G-COOH and its future applications.

Received 4th May 2015,
Accepted 30th August 2015

DOI: 10.1039/c5tx00137d

www.rsc.org/toxicology

Introduction

Graphene, a single- or few-layered sheet of sp^2-bonded carbon atoms, is a nanomaterial that has attracted tremendous attention due to its unique physico-chemical properties.[1] Previous studies have indicated that pristine graphene and some members of the graphene family such as graphene oxide (GO) have toxic effects on organisms.[2–5] Since a biocompatibility is a main concern for the actual application of engineered nanomaterials (ENMs) in biology and in medicine, some specific surface functionalizations have been used to modify graphene with the goal of making it less harmful to organisms.[1,5] Carboxyl functionalization can be achieved by mild acid treatment, which results in the addition of COOH groups at the surface. This end product is referred to as the carboxyl functionalized graphene (G-COOH).[4] G-COOH has a similar chemical structure to GO, except that it has a higher carboxyl ratio and additional ethanoic acid groups on the sp^3-hybridized carbon on the basal plane.[6] The modified graphene, G-COOH, can potentially be useful for biosensing and medical applications.[7–10]

So far, only limited studies on the *in vitro* toxicity assessment of G-COOH have been reported. Using monkey kidney Vero cells as an assay system, it has been reported that G-COOH could be internalized by cells without causing any toxicity.[4] However, it has been reported that in the human hepatocellular carcinoma Hep G2 cell line, G-COOH caused structural damage on the plasma membrane and induced an increase in intracellular reactive oxygen species (ROS) at a concentration as low as 4 μg mL^{-1}.[6] Therefore, contradictory conclusions have been obtained from the *in vitro* studies on G-COOH toxicity. Moreover, we know little about the *in vivo* behavior and toxicity of G-COOH.

[a]*Key Laboratory of Environmental Medicine Engineering in Ministry of Education, Medical School of Southeast University, Nanjing 210009, China. E-mail: dayongw@seu.edu.cn; Tel: +86-25-83272510*
[b]*College of Life Sciences and Engineering, Chongqing Three Gorges University, Wanzhou 404000, China*
[c]*Institute of Nanochemistry and Nanobiology, Shanghai University, Shanghai 200444, China*
†Electronic supplementary information (ESI) available. See DOI: 10.1039/c5tx00137d
‡They contributed equally to this work.

The potential of *Caenorhabditis elegans* as a model organism was first recognized by Brenner.[11] *C. elegans*, a free-living soil nematode, is an animal model with a short lifespan and a well-defined anatomy. *C. elegans* is also easy to be manipulated and cheap to be maintained. *C. elegans* has been considered as an important assay system for toxicological studies because of its high sensitivity to various stresses or toxicants.[12–16] Multiple toxicity assessments and toxicological studies of carbon-based ENMs have been performed using *C. elegans*.[17–20] *C. elegans* can be further used to study the distribution and translocation of carbon-based ENMs such as multi-walled carbon nanotubes (MWCNTs) and GO.[21–26]

It has been reported that graphite nanoplatelets had no toxic effects on *C. elegans*.[27] However, others have shown that GO caused adverse effects on the functions of both the primary targeted organs such as the intestine and the secondary targeted organs such as neurons and reproductive organs in nematodes.[23] GO could be translocated into the body of nematodes through the intestinal barrier.[23,28] In the present study, we examined the cellular basis for *in vivo* translocation and toxicity of G-COOH using *C. elegans* as an assay system. Our results demonstrate the *in vivo* effects of G-COOH, and the biodistribution of G-COOH in nematodes. Moreover, our data suggest the crucial roles of the intestinal barrier and defecation behavior in preventing the accumulation and toxicity of G-COOH in nematodes. Our results provide important insights into the *in vivo* behavior and toxicity of G-COOH.

Results and discussion

Characterization of G-COOH

The atomic force microscopy (AFM) image shows that the height of G-COOH was between 1.69 and 2.01 nm, implying the two carbon layers (Fig. 1a). Based on the size of 2-D particles, most of the G-COOH in K-medium was in the range of 40–50 nm after the sonication (Fig. 1b). The G-COOH aggregate size was 129 ± 43 nm in K medium. The Fourier transform infrared (FTIR) spectrum of G-COOH confirmed the presence of the COOH group in the graphene. In the FTIR spectrum the peak at 3398 cm^{-1} is attributed to O–H stretching vibration, the peak at 1700 cm^{-1} is attributed to C═O stretching vibration, the peak at 1625 cm^{-1} is attributed to the vibration of C═C, and the peak at 1050 cm^{-1} is attributed to the vibration of C–O (alkoxy) (Fig. 1c). The Raman spectra of G-COOH showed the existence of both the D (1345 cm^{-1}) band and G (1593 cm^{-1}) band (Fig. 1d). The obtained G-COOH had a zeta-potential of −23.2 ± 1.1 mV in K medium.

Effects of prolonged exposure to G-COOH on nematodes

Prolonged exposure from L1-larvae to adult day-1 (approximately 4 days) was performed. We selected GO as the control ENM having adverse effects on nematodes.[23,28] The sizes of most of the GO in K medium were in the range of 40–50 nm. The GO aggregate size was 154 ± 34 nm in K medium. The zeta potential of GO in K medium was −22.5 ± 1.4 mV. The exam-

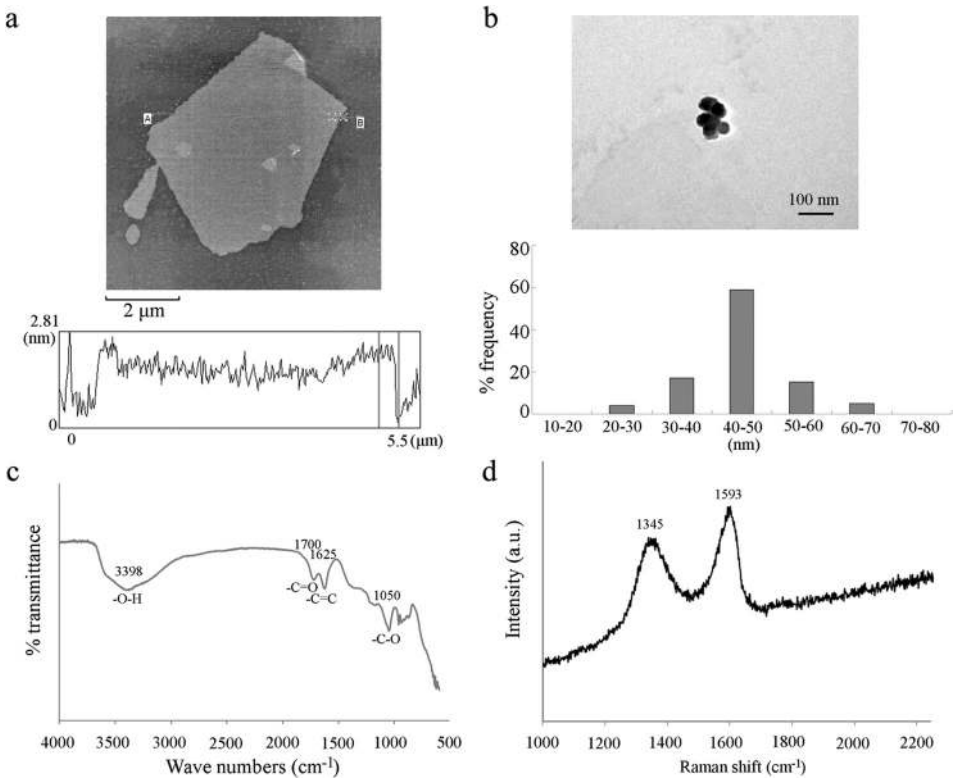

Fig. 1 Physicochemical properties of the prepared G-COOH. (a) AFM of G-COOH. (b) TEM image of G-COOH in K-medium after sonication. (c) FTIR spectrum of G-COOH. (d) Raman spectrum of G-COOH.

ined concentrations of G-COOH were 0.01–100 mg L^{-1}. After prolonged exposure, G-COOH at all the examined concentrations did not cause any obvious effects on the lifespan of nematodes compared with the control (Fig. 2a). Similarly, G-COOH at all the examined concentrations did not significantly affect the body length of nematodes compared with the control (Fig. 2b). In contrast, prolonged exposure to GO (100 mg L^{-1}) obviously reduced the lifespan and decreased the body length of nematodes (Fig. 2a and b).

In nematodes, the toxic ENMs might adversely affect the functions of both the primary targeted organs such as the intestine and the secondary targeted organs such as neurons and reproductive organs.[15] We could not detect the significant induction of intestinal ROS production in nematodes exposed to all the examined concentrations of G-COOH (Fig. 2c). In contrast, prolonged exposure to GO (100 mg L^{-1}) significantly induced the intestinal ROS production compared with the control (Fig. 2c). Moreover, we did not observe any significant changes of locomotion behavior as reflected by the endpoints of body bend and head thrash in nematodes exposed to the examined concentrations of G-COOH (Fig. 2d). Similarly, prolonged exposure to all the examined concentrations of G-COOH did not significantly decrease the brood size of nematodes (Fig. 2e). In contrast, prolonged exposure to GO (100 mg L^{-1}) significantly decreased both the locomotion behavior and the brood size of nematodes compared with the control (Fig. 2d and e). These data suggest that nematodes exposed to the examined concentrations of G-COOH could maintain the normal physiological functions of certain targeted organs.

Effects of prolonged exposure to G-COOH on the progeny of the exposed nematodes

We next investigated the effects of G-COOH on the filial generation (F1) of the exposed nematodes (P0). In the progeny of G-COOH (1–100 mg L^{-1}) exposed nematodes, we did not detect any noticeable alteration in both the lifespan and the body length of nematodes (Fig. 3a and b). Moreover, we did not observe the significant induction of intestinal ROS production in the progeny of G-COOH (1–100 mg L^{-1}) exposed nematodes (Fig. 3C). Furthermore, no significant decrease in locomotion

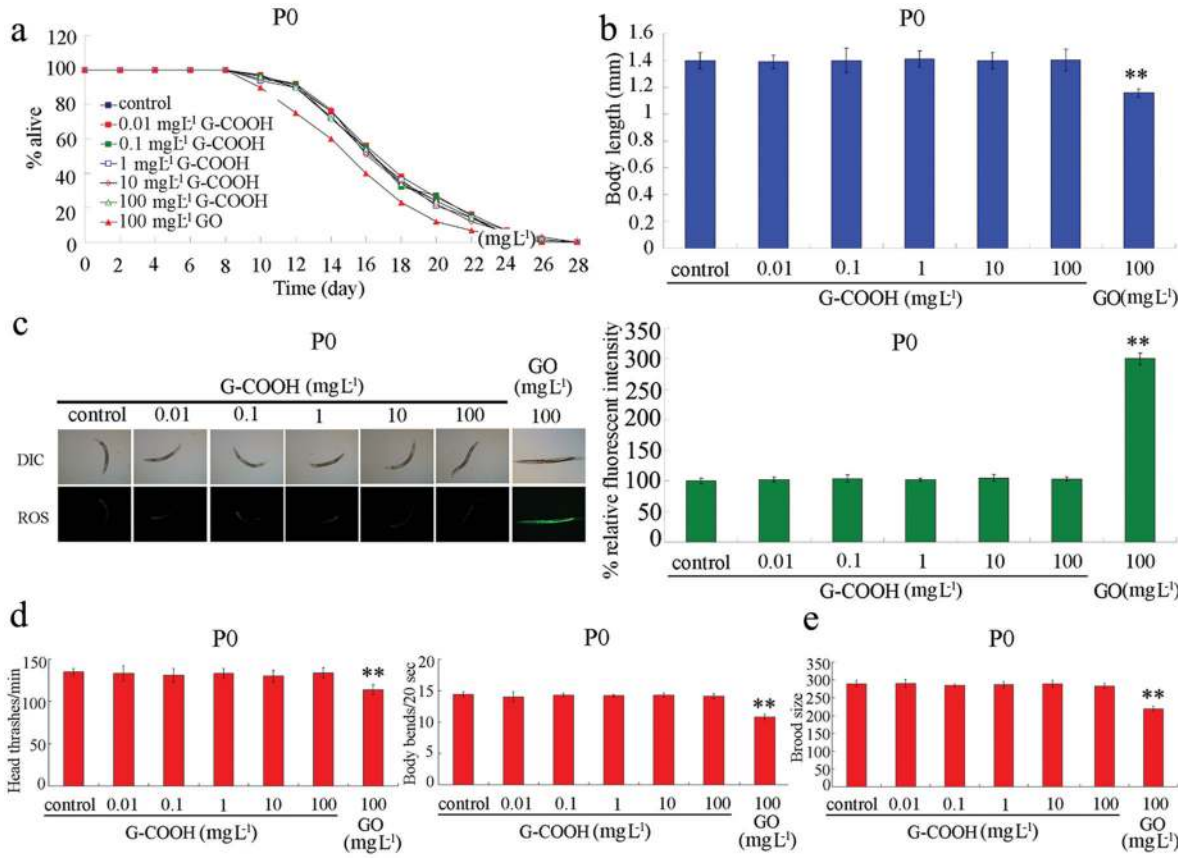

Fig. 2 Effects of prolonged exposure to G-COOH on animals. (a) Effects of G-COOH on the lifespan of nematodes. Forty nematodes were examined per treatment. (b) Effects of G-COOH on the body length of nematodes. Thirty nematodes were performed per treatment. (c) Effects of G-COOH on the induction of intestinal ROS production. The left shows the pictures, and the right shows the comparison of the relative fluorescence intensity in the intestine. Fifty nematodes were examined per treatment. (d) Effects of G-COOH on locomotion behavior (head thrash and body bend) in nematodes. Twenty nematodes were examined per treatment. (e) Effects of G-COOH on the brood size of nematodes. Twenty nematodes were examined per treatment. Prolonged exposure was performed from L1-larvae to adult day-1. Bars represent means ± SEM. $^{**}P < 0.01$.

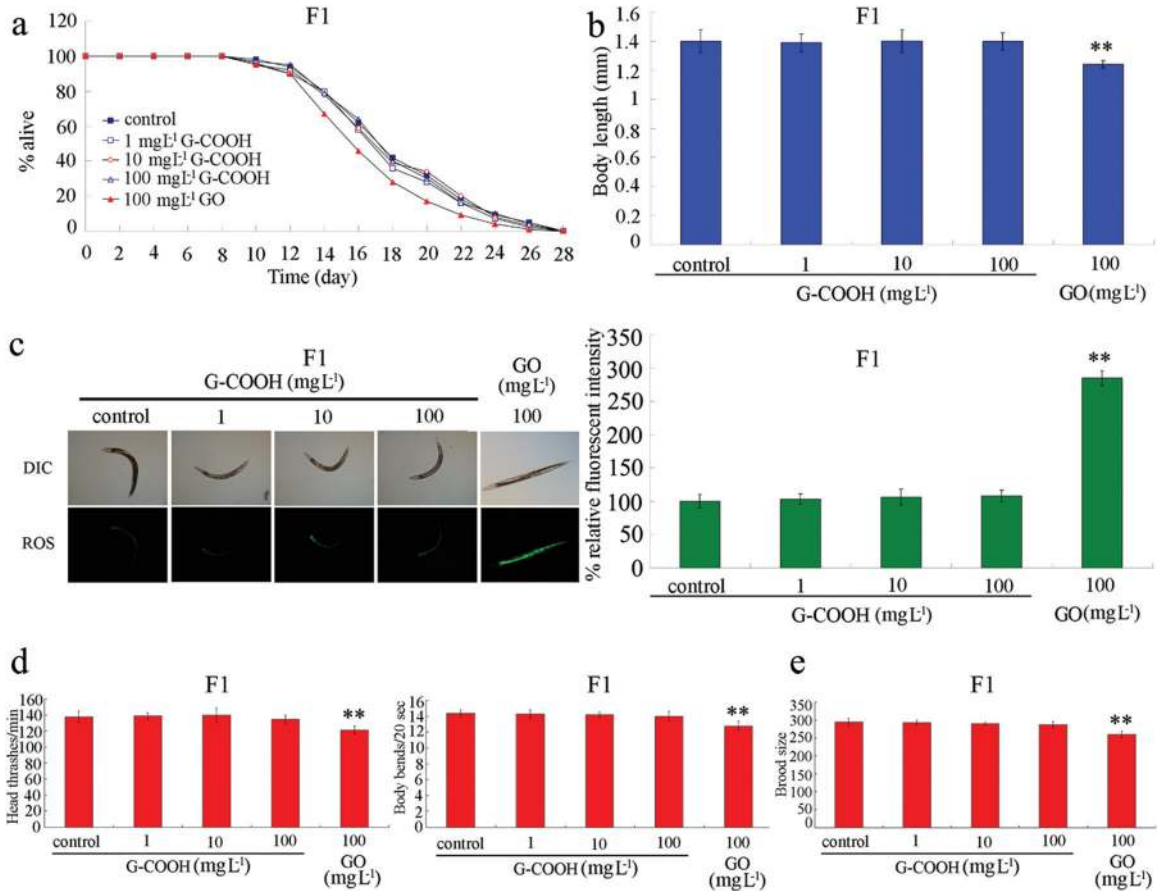

Fig. 3 Phenotypic analysis in the progeny of animals exposed to G-COOH. (a) Lifespan in the progeny of animals exposed to G-COOH. Forty nematodes were examined per treatment. (b) Body length in the progeny of animals exposed to G-COOH. Thirty nematodes were performed per treatment. (c) Intestinal ROS production in the progeny of animals exposed to G-COOH. The left shows the pictures, and the right shows the comparison of the relative fluorescence intensity in the intestine. Fifty nematodes were examined per treatment. (d) Locomotion behavior (head thrash and body bend) in the progeny of animals exposed to G-COOH. Twenty nematodes were examined per treatment. (e) Brood size in the progeny of animals exposed to G-COOH. Twenty nematodes were examined per treatment. Prolonged exposure was performed from L1-larvae to adult day-1. Bars represent means ± SEM. $^{**}P < 0.01$.

behavior or reduction in the brood size was detected in the progeny of 1–100 mg L^{-1} of G-COOH exposed nematodes (Fig. 3d and e). In contrast, in the progeny of the GO (100 mg L^{-1}) exposed nematodes, we observed an obvious reduction in lifespan, induction of intestinal ROS production, and a decrease in body length, locomotion behavior or brood size (Fig. 3). These data further suggest the normal physiological functions of the intestine, neurons, and reproductive organs in the progeny of the G-COOH exposed nematodes.

Distribution and translocation of G-COOH in nematodes

To determine the cellular mechanism for the effects of G-COOH on nematodes, we investigated the distribution and translocation of G-COOH/Rhodamine B (Rho B). After prolonged exposure, we found that G-COOH/Rho B (100 mg L^{-1}) was mainly distributed in the pharynx and intestine of nematodes (Fig. 4a). We could not observe the distribution of G-COOH/Rho B in the secondary targeted organs such as the reproductive organ like gonads (Fig. 4a and S2†). Moreover, we could not detect the obvious signals for G-COOH/Rho B in the progeny of nematodes exposed to 100 mg L^{-1} of G-COOH/Rho B (Fig. 4b). In contrast, GO could be distributed in the pharynx, intestine, and reproductive organs such as gonads in nematodes exposed to 100 mg L^{-1} of GO.[26] Moreover, we could also detect the GO distribution in the pharynx, intestine, and gonad in the progeny of nematodes exposed to 100 mg L^{-1} of GO (Fig. S1†). Compared with the distribution of G-COOH/Rho B and that of GO/Rho B in nematodes, exposure to Rho B alone caused a relatively equal distribution of fluorescence in tissues of nematodes (Fig. S3†). These results suggest that G-COOH may be confined to the intestine and cannot be translocated into the secondary targeted organs through the intestinal barrier in nematodes.

Biodistribution of G-COOH in the intestinal cells of nematodes

With the aid of some transgenic strains, we further examined the biodistribution of G-COOH in specific organelles within

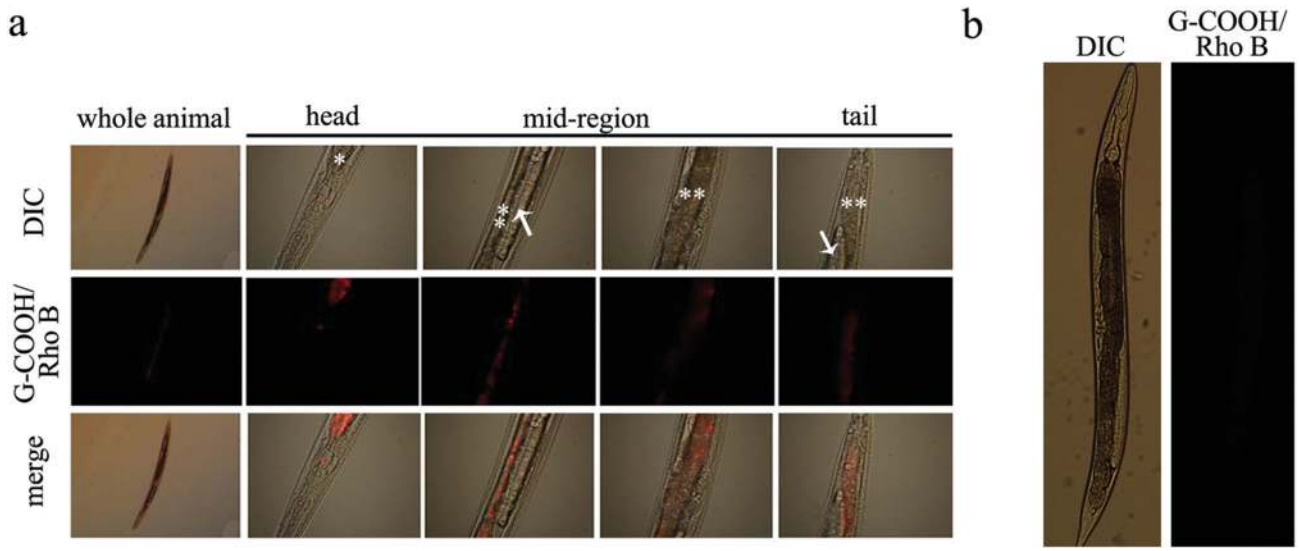

Fig. 4 Distribution and translocation of G-COOH in exposed nematodes and their progeny. (a) Distribution and translocation of G-COOH in exposed nematodes. (b) Distribution and translocation of G-COOH in the progeny of exposed nematodes. Prolonged exposure was performed from L1-larvae to adult day-1. The exposure concentration of G-COOH was 100 mg L^{-1}. The arrowheads indicate the gonad at the mid-region of nematodes. The pharynx (*) and the intestine (**) are also indicated.

the intestinal cells of nematodes. In the transgenic strain of *zcIs18*, green fluorescent protein (GFP) is expressed in the cytosol of intestinal cells of nematodes. We observed a moderate biodistribution of G-COOH in the cytosol of intestinal cells in the anterior, mid-, and posterior regions of the *zcIs18* nematodes (Fig. 5). In the transgenic strain of *zcIs17*, GFP is expressed in the mitochondria of intestinal cells of nematodes. We did not observe the obvious biodistribution of G-COOH in the mitochondria of intestinal cells of the *zcIs17* nematodes (Fig. 5). In the transgenic strain of *hiIs8*, GFP is expressed in the peroxisome of intestinal cells of nematodes. We detected a large amount of G-COOH biodistribution in the peroxisome of intestinal cells in the anterior and mid-regions of the *hiIs8* nematodes (Fig. 5). In the transgenic strain of *hiIs9*, GFP is expressed in the lysosome of intestinal cells of nematodes. We found a large amount of G-COOH biodistribution in the lysosome of intestinal cells in the mid-region and posterior region of the *hiIs9* nematodes (Fig. 5). Therefore, after prolonged exposure, we found that G-COOH can be deposited in the specific subcellular compartments of intestinal cells in nematodes.

To confirm the subcellular distribution of G-COOH in the intestinal cells, we employed the transmission electron microscopy (TEM) technique. We observed that G-COOH could be translocated into the intestinal cells, and mainly deposited in the small-vesicle structures adjacent to the intestinal microvilli (Fig. 6). A moderate amount of G-COOH was also observed to be distributed in the cytosol of intestinal cells (Fig. 6). Occasionally, the G-COOH was also found in some large-vesicle structures in the cytosol of intestinal cells (Fig. 6). However, no G-COOH was found in the mitochondria of intestinal cells (Fig. 6). Meanwhile, we found that a large amount of G-COOH was deposited in the intestine along with food particles (Fig. 6). We did not observe the obvious distribution of G-COOH in germ cells in gonads, muscles, and excretory canals of nematodes (Fig. S4†). In contrast, after prolonged exposure, GO was found to be mainly distributed adjacent to or surrounding mitochondria in the cytosol of intestinal cells.[22] In contrast to the disrupted ultrastructure of microvilli and the loss of many microvilli on intestinal cells observed in the GO exposed nematodes,[22] no developmental deficit in intestinal cells was observed in the G-COOH exposed nematodes (Fig. 6).

Effects of prolonged G-COOH exposure on the expression pattern of genes required for the control of oxidative stress

We next investigated the effects of G-COOH exposure on the expression pattern of genes required for the control of oxidative stress in nematodes. After prolonged exposure to 100 mg L^{-1} of G-COOH, we found that the expression levels of *sod-2*, *sod-3*, *mev-1*, *clk-1*, *gas-1*, and *isp-1* genes in the G-COOH exposed nematodes were similar to those in control nematodes (Fig. S5 and S6, Table S1†). In *C. elegans*, *sod-2* and *sod-3* genes encode the mitochondria manganese-superoxide dismutase, the *mev-1* gene encodes a subunit of the mitochondrial respiratory chain complex II (a subunit of the enzyme succinate dehydrogenase cytochrome b), the *isp-1* gene encodes a subunit of the mitochondrial complex III ("Rieske" iron–sulfur protein), the *gas-1* gene encodes a subunit of mitochondrial complex I, and the *clk-1* gene encodes a ubiquinone biosynthesis protein COQ7. Therefore, despite the moderate deposition of G-COOH in intestinal cells, no noticeable alterations of the expression pattern of genes required for the control of oxidative stress were observed in nematodes. Moreover, our

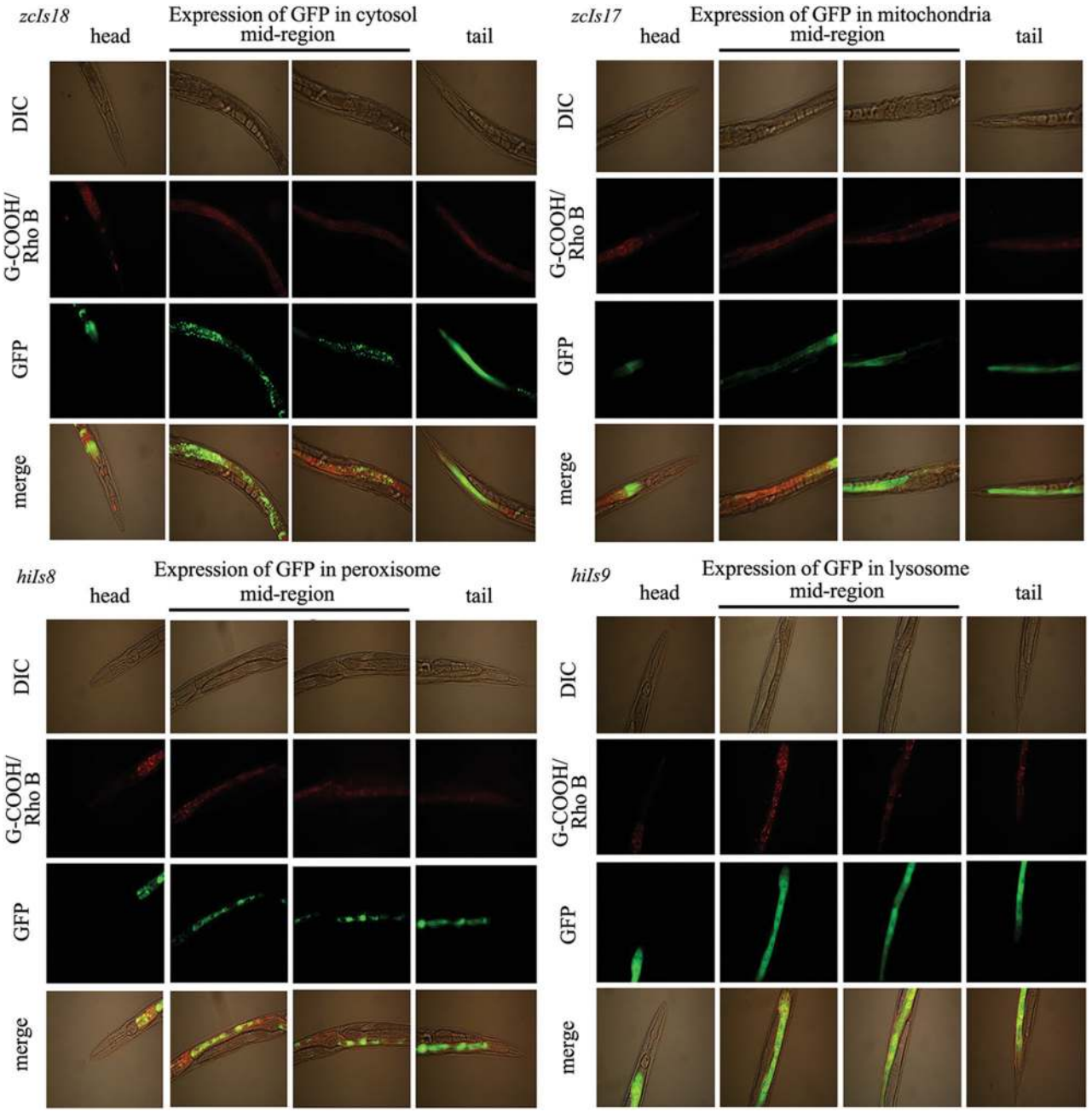

Fig. 5 Biodistribution of G-COOH in the cytosol, mitochondria, peroxisome, and lysosome of the intestinal cells in nematodes. Prolonged exposure was performed from L1-larvae to adult day-1. The exposure concentration of G-COOH/Rho B was 100 mg L^{-1}.

data imply that the moderate deposition of G-COOH in the cytosol and in certain organelles of intestinal cells does not alter the mitochondrial functions in the intestinal cells of nematodes.

Prolonged exposure to G-COOH did not alter the intestinal permeability

Considering the important role of the primary targeted organs in the translocation and distribution of ENMs, we investigated the intestinal permeability in G-COOH exposed nematodes. We employed the lipophilic fluorescent dye Nile Red to stain the G-COOH exposed nematodes. Compared with the control, prolonged exposure to 0.01–100 mg L^{-1} G-COOH did not obviously affect the relative fluorescence intensity of Nile Red in the intestines of nematodes (Fig. 7a). Similarly, the relative fluorescence intensity of Nile Red in the intestines of the progeny of the G-COOH exposed nematodes was the same as that of the control (data not shown). In contrast, prolonged

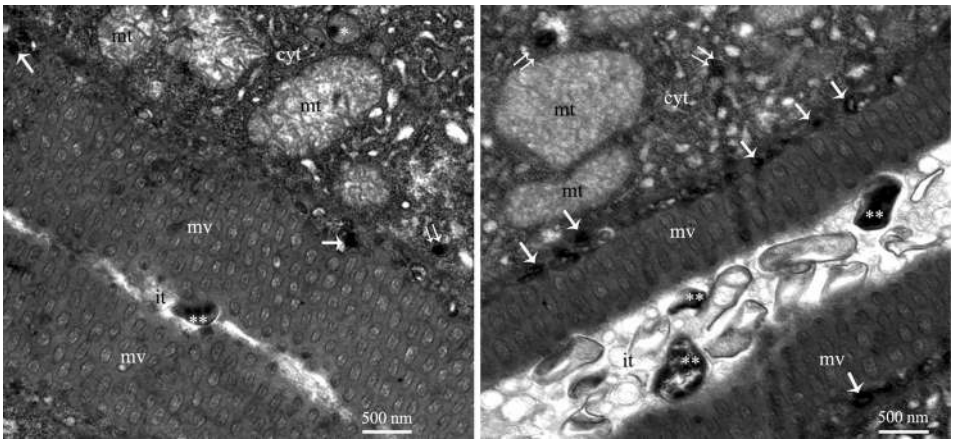

Fig. 6 Subcellular distribution of G-COOH in the intestinal cells of nematodes. mt, mitochondria; cyt, cytosol; mv, microvilli; it, intestine. Prolonged exposure was performed from L1-larvae to adult day-1. The exposure concentration of G-COOH was 100 mg L^{-1}. Single-arrowheads indicate the distribution of G-COOH in the small-vesicle structures adjacent to the intestinal microvilli. Double-arrowheads indicate the distribution of G-COOH in the cytosol of intestinal cells. Double-asterisks indicate the food particles in the intestine.

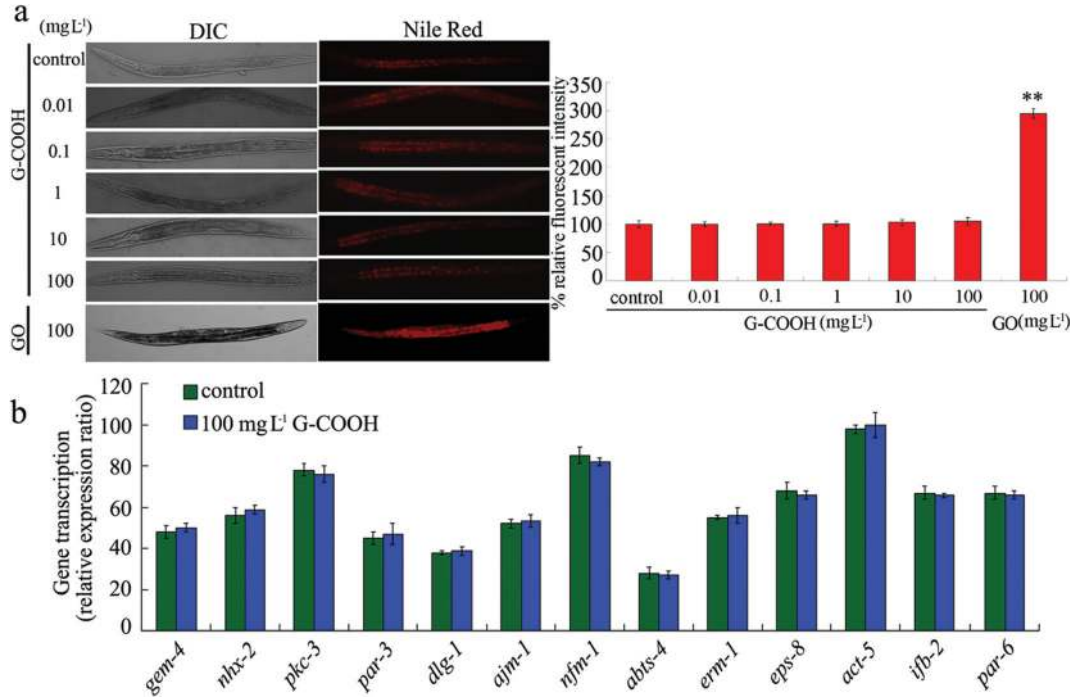

Fig. 7 Effects of G-COOH exposure on the intestinal permeability in *C. elegans*. (a) Comparison of the relative fluorescence intensities of Nile Red in nematodes exposed to G-COOH. The left shows the pictures, and the right shows the comparison of the relative fluorescence intensity in the intestine. Twenty nematodes were examined per treatment. (b) The expression pattern comparison of genes required for the intestinal development in nematodes exposed to 100 mg L^{-1} of G-COOH using the method of qRT-PCR. The final results are expressed as the relative expression ratio (between the targeted gene and the *tba-1* reference gene). Prolonged exposure was performed from L1-larvae to adult day-1. Bars represent means ± SEM. $^{**}P < 0.01$.

exposure to GO (100 mg L^{-1}) caused a significant increase in Nile Red staining in the intestine of the exposed nematodes (Fig. 7a). These data imply that prolonged exposure to G-COOH may not affect the permeability of the intestinal barrier in nematodes.

Prolonged exposure to G-COOH did not alter the expression patterns of genes required for intestinal development

We further investigated the expression patterns of genes required for intestinal development (Table S2†) in the

G-COOH exposed nematodes. After prolonged exposure to 100 mg L^{-1} G-COOH, we found no obvious alterations in the expression patterns of *gem-4*, *nhx-2*, *pkc-3*, *par-3*, *par-6*, *dlg-1*, *ajm-1*, *nfm-1*, *abts-4*, *erm-1*, *eps-8*, *act-5*, and *ifb-2* genes in the exposed nematodes (Fig. 7b and S6, Table S1†). In *C. elegans*, *gem-4*, *nhx-2*, *pkc-3*, *par-3*, *par-6*, *erm-1*, *eps-8*, *act-5*, and *ifb-2* genes are required for the development of microvilli on intestinal cells; *nfm-1* and *abts-4* genes are required for the development of the basolateral domain of the intestine; and *dlg-1* and *ajm-1* genes are associated with the development of the apical junction of the intestine.[29] In contrast, prolonged exposure to GO (100 mg L^{-1}) significantly increased the expression level of the *nhx-2* gene and decreased the expression levels of *par-6* and *pkc-3* genes.[22] Our results imply that prolonged exposure to G-COOH may not noticeably affect the various aspects of intestinal development in nematodes.

Prolonged exposure to G-COOH did not change defecation behavior and structure of neurons regulating defecation behavior

Besides the normal permeable state of the intestinal barrier, another possibility that could explain the observed limited effects of G-COOH on nematodes is the maintenance of normal defecation behavior. Defecation is the behavior of nematodes to undergo a stereotypic pattern of muscle contractions ultimately leading to the expulsion of intestinal contents. We found that prolonged exposure to 0.01–100 mg L^{-1} G-COOH could not significantly affect the mean defecation cycle length in the exposed nematodes compared with the control (Fig. 8a). In contrast, prolonged exposure to 100 mg L^{-1} of GO induced a significant increase in mean defecation cycle length (Fig. 8a). The mean defecation cycle length in the progeny of G-COOH exposed nematodes was also similar to that of control nematodes (data not shown).

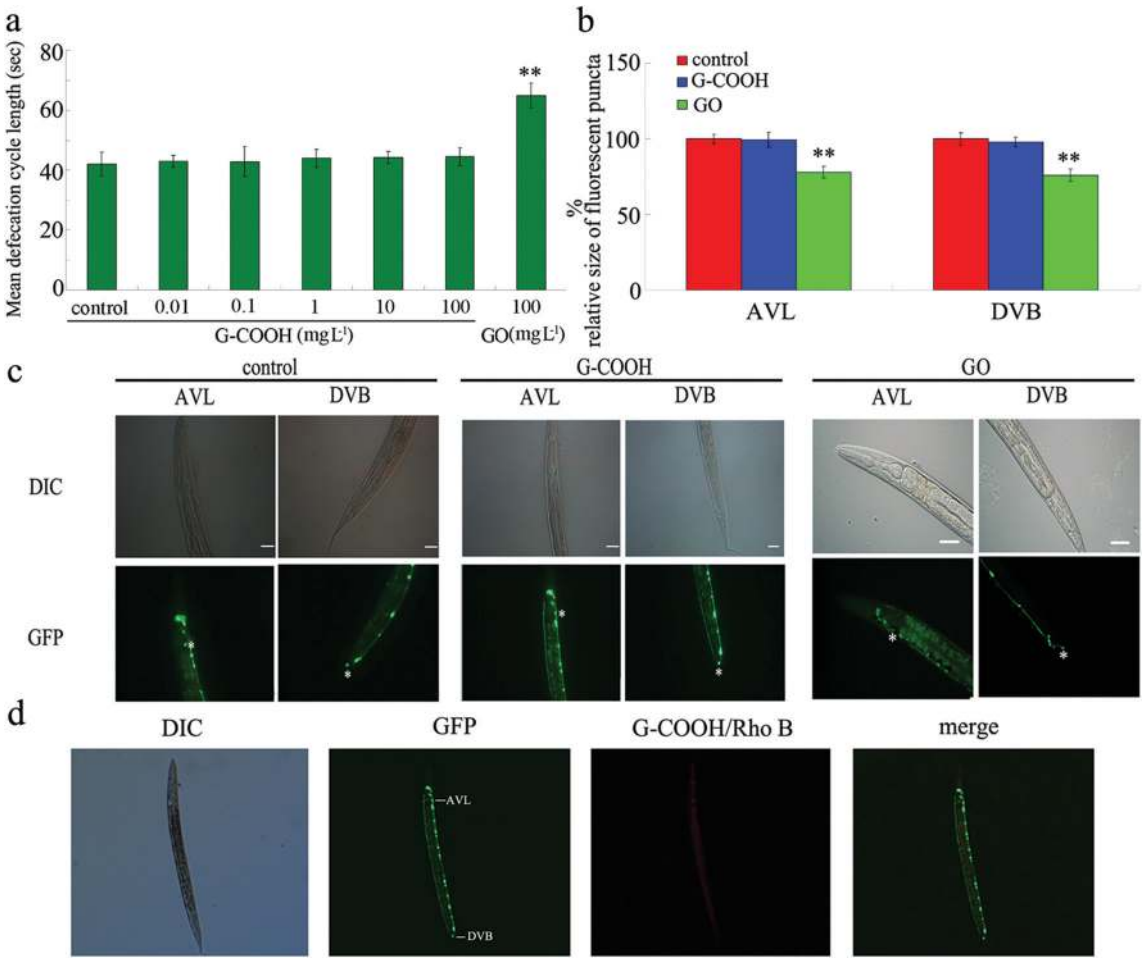

Fig. 8 Effects of G-COOH exposure on defecation behavior. (a) Effects of G-COOH exposure on the mean defecation cycle length. Thirty nematodes were examined per treatment. (b) Effects of exposure to 100 mg L^{-1} of G-COOH on the relative size of fluorescent puncta of AVL or DVB neurons. Twenty nematodes were examined per treatment. (c) Effects of exposure to 100 mg L^{-1} of G-COOH on the development of AVL or DVB neurons. The neurons (*) were indicated. Scale bars represent 30 μm. (d) Colocalization assay of G-COOH/Rho B with GABAergic neurons. The exposure concentration for G-COOH was 100 mg L^{-1}. Prolonged exposure was performed from L1-larvae to adult day-1. Bars represent means ± SEM. $^{**}P < 0.01$.

In *C. elegans*, defecation behavior is controlled by AVL and DVB neurons.[30] To further investigate the possible structural alterations of AVL and DVB neurons, we employed a transgenic strain *oxIs12* which contains labeled AVL and DVB neurons in the GABAergic nervous system. We observed that the structures of both AVL and DVB neurons remained relatively unchanged in nematodes exposed to 100 mg L^{-1} of G-COOH (Fig. 8b and c). In contrast, prolonged exposure to 100 mg L^{-1} of GO caused a reduction in the relative size of fluorescent puncta in the cell bodies of AVL or DVB neurons (Fig. 8c).

We also found that G-COOH/Rho B could not be translocated into the GABAergic nervous system including the AVL and DVB neurons (Fig. 8d). Therefore, both the permeable state of the intestinal barrier and the defecation state may contribute greatly to the extent of potential effects of G-COOH on nematodes.

Chronic exposure to G-COOH did not cause adverse effects on nematodes

We finally investigated the effects of chronic exposure to G-COOH from L1-larvae to adult day-10 (approximately 13 days) on nematodes with the endpoint of locomotion as the endpoints. After chronic exposure, G-COOH (100 mg L^{-1}) did not cause obvious adverse effects on the locomotion behavior of nematodes compared with the control (Fig. S7†). In contrast, chronic exposure to GO (1 mg L^{-1}) significantly decreased the locomotion behavior of nematodes (Fig. S7†).

In the present study, we focused on G-COOH, a graphene derivative, to investigate its possible environmental friendliness. The G-COOH used in our experiments may contain two carbon layers (Fig. 1a). The zeta potential of G-COOH in K-medium was −23.2 ± 1.1 mV, which implies the possible stablity of G-COOH in K-medium. The size of assayed G-COOH in K-medium was in the range of 40–50 nm (Fig. 1b), which suggests its potential in the aspect of drug delivery. The diameter of the pharynx in *C. elegans* is approximately 20 μm at its widest (at the posterior bulb), which is another reason for selecting the G-COOH with small sizes (40–50 nm).

Using *C. elegans* as an *in vivo* assay system, we performed toxicity assessment of G-COOH. We exposed nematodes to G-COOH from L1-larvae to adult day-1 to examine the effects of prolonged exposure to G-COOH on nematodes. Our data demonstrate that prolonged exposure to 0.01–100 mg L^{-1} of G-COOH could not noticeably affect the lifespan and development of nematodes (Fig. 2a and b). Moreover, prolonged exposure to the examined concentrations of G-COOH did not significantly induce intestinal ROS production or alter both the locomotion behavior and the brood size (Fig. 2c–e). Furthermore, chronic exposure to 100 mg L^{-1} of G-COOH from L1-larvae to adult day-10 did not noticeably affect the locomotion behavior (Fig. S7†). This implies that G-COOH exposed nematodes may maintain normal functions of the targeted organs. Our *in vivo* assay data are consistent with the observations of G-COOH performance in the monkey kidney Vero cell line to a certain degree.[4] The differences between our study and previous studies could be explained by the fact that toxicants are usually considered bioavailable for nematodes because testing solutions are fed directly into the intestine. A previous study has suggested that G-COOH at concentrations of more than 4 mg L^{-1} could cause structural damage to Hep G2 cells.[6] Therefore, the relatively high G-COOH concentrations used in this study might be available for the intestinal barrier of nematodes. Previous studies have further suggested that negatively charged COO^- modified ENMs may be far less toxic than positively charged NH_3^+ modified ENMs.[31,32]

Besides the effects of G-COOH on exposed nematodes, we also examined the effects of G-COOH on the progeny of exposed nematodes. We did not detect any obvious alterations in both the lifespan and development in the progeny of nematodes exposed to 1–100 mg L^{-1} of G-COOH (Fig. 3a and b). Similarly, we did not observe any significant induction of intestinal ROS production or any noticeable changes of locomotion behavior and brood size in the progeny of nematodes exposed to 1–100 mg L^{-1} of G-COOH (Fig. 3c–e). These results suggest that the normal functions of the intestine, neurons, and reproductive organs are maintained in the progeny of the G-COOH exposed nematodes. These data also imply that G-COOH may not be able to induce toxicity in exposed nematodes that would be amplified in the next generation.

In this study, we observed the different effects between GO and G-COOH on nematodes. This difference is to a certain degree due to the difference in chemical properties between GO and G-COOH. The crystallization state of graphene can be reflected by the ratio of G band peak to D band peak ($R = I_G/I_D$) in its Raman spectroscopy. The higher ratio means the more perfect crystallization. In Raman spectroscopy,[23] the R value of G-COOH was more than that of GO. The COOH and OH contents in GO and G-COOH were also measured by X-ray photoelectron spectroscopy (XPS). The C 1s spectra of G-COOH and GO were analyzed and the results are summarized in Table S3.† Clearly, GO contains more oxygen than G-COOH, according to the C/O ratio (Table S3†). The content of COOH in GO is 2.13%, which is higher than that in G-COOH (1.41%) (Table S3†). As for the OH group, it is 50.35% in GO and 51.35% in G-COOH (Table S3†). This property implies that more oxygen-containing groups may exist on GO, which may further cause more adverse effects on cells or organisms compared with G-COOH.

In *C. elegans*, ENMs have been suggested to be translocated into both the primary and the secondary targeted organs.[15,33,34] For the underlying cellular mechanism of the *in vivo* effects of G-COOH on nematodes, one of the crucial explanations may be the translocation pattern of G-COOH in nematodes. After prolonged exposure, we found that G-COOH could not be translocated into the reproductive organs such as gonads in exposed nematodes (Fig. 4a). G-COOH was also not found in GABAergic neurons (Fig. 8d). That is, G-COOH was not bioavailable for both the neurons and the reproductive organs in G-COOH exposed nematodes. This translocation pattern of G-COOH may explain the maintenance of normal functions of both neurons and reproductive organs in G-COOH exposed nematodes. Moreover, we did not detect the

distribution of G-COOH in the progeny of exposed nematodes (Fig. 4b), which explained the normal developmental state in the progeny of nematodes exposed to G-COOH. Similarly, we suppose that G-COOH may not be able to induce the obvious toxicity on the targeted organs, if no enough amount of G-COOH can be deposited in the targeted organs after crossing the corresponding biological barrier in the mammals.

After prolonged exposure, we found that G-COOH could be moderately distributed in the cytosol and some organelles such as peroxisomes and lysosomes in the exposed nematodes (Fig. 5). A previous study has suggested that G-COOH had the high affinity for the membrane and could penetrate through the cell membrane into the cytosol where it is concentrated and enclosed in vesicles.[6] In cells, peroxisomes are involved in the reduction of reactive oxygen species specifically hydrogen peroxide.[35] Different from this, lysosomes act as the waste disposal system by digesting unwanted materials in the cytoplasm and are responsible for cellular homeostasis by participating in the plasma membrane repair in cells.[36] In contrast, G-COOH was seldom distributed in mitochondria (Fig. 5). Meanwhile, we did not detect the significant induction of intestinal ROS production in G-COOH exposed nematodes (Fig. 2c). This is partially reflected by the normal expression patterns of genes required for control of oxidative stress in the G-COOH exposed nematodes (Fig. S5†). A previous study has suggested the important roles of the bioavailablility of ENMs to mitochondria in the disturbance of the mitochondrial membrane and in the induction of oxidative stress.[37] In this study, the fact that no noticeable induction of ROS production in intestinal cells was found may be largely due to the unavailability of G-COOH to mitochondria in the cytosol of intestinal cells. That is, the deposited amount of G-COOH within other compartments of intestinal cells may be not enough to induce toxic effects on the development of intestinal cells. It could also be that the distribution pattern of G-COOH within intestinal cells may not align with what is required for inducing oxidative stress in intestinal cells.

Another possible explanation to the limited *in vivo* effects of G-COOH on nematodes is the normal functional state of the intestine. Besides the absence of induction of intestinal ROS production, we also observed normal intestinal development and intestinal permeability in G-COOH exposed nematodes (Fig. 6 and 7a). Moreover, the expression patterns of genes required for intestinal development were not significantly altered in G-COOH exposed nematodes (Fig. 7b). These data further imply that the amount of deposited G-COOH in the intestine may not be enough to affect the development and function of the intestinal barrier. The normal biological function of the intestinal barrier may effectively prevent the translocation of G-COOH into other organs in exposed nematodes. G-COOH was mainly deposited in the small-vesicle structures adjacent to microvilli of intestinal cells (Fig. 6). The deposited G-COOH in intestinal cells did not appear to be transported out of the intestinal cells. Our data further support the crucial role of the intestinal barrier on the protection of animals from the toxic effects of toxicants such as ENMs.[21–24] Although our results do not completely eliminate the possible adverse effects of G-COOH, they imply that at the examined concentrations, G-COOH did not cause toxic effects on nematodes, potentially due to the presence of biological barriers.

The observed normal state of defecation behavior in the G-COOH exposed nematodes could also be a potential explanation for the limited *in vivo* effects of G-COOH on nematodes. After prolonged exposure, G-COOH exposed nematodes displayed normal defection behavior and normal development of AVL and DVB neurons, which are involved in controlling defecation behavior (Fig. 8a–c). Therefore, one of the reasons for the moderate amount of G-COOH deposition in intestinal cells may be that most of the G-COOH was excreted from the body of the exposed nematodes. The absence of colocalization of G-COOH/Rho B with AVL or DVB neurons (Fig. 8d) may explain the normal development and function of AVL and DVB neurons in the G-COOH exposed nematodes.

Conclusions

In conclusion, we investigated the *in vivo* effects of G-COOH using *C. elegans* as an assay system. Our data demonstrate that G-COOH in the range of mg L^{-1} did not cause toxic effects on both the exposed nematodes and their progeny. Although a moderate amount of G-COOH was deposited in the cytosol and some organelles of intestinal cells, no G-COOH was found to be translocated into neurons or reproductive organs, as well as in the body of the progeny of exposed nematodes. The moderate deposition of G-COOH did not induce toxic effects on the development and function of intestinal cells. We conclude that the G-COOH translocation pattern, the normal function of the intestinal barrier, and the normal defecation behavior contribute greatly to the extent of observed *in vivo* effects of G-COOH on nematodes.

Experimental

Characterization of G-COOH

G-COOH was from Nanjing Jcnano Tech. Co., Ltd. For the physico-chemical characterization of G-COOH, TEM, AFM, FTIR, and Raman spectroscopy were performed. After sonication, the morphology and size distribution of G-COOH in K-medium (51 mmol L^{-1} NaCl, and 32 mmol L^{-1} KCl) were examined by TEM. TEM images were recorded on a JEM-200CX field emission electron microscope, equipped with a cooled charge-coupled device (CCD) camera. A few drops of G-COOH suspension solution were deposited on the TEM grid, dried, and evacuated before analysis. The zeta potential of G-COOH or GO in K-medium was analyzed with a Nano Zetasizer using a dynamic light scattering technique. GO was synthesized according to the modified Hummer's method.[38] The physico-chemical characterization by TEM, AFM, FTIR, and Raman spectroscopy of GO has been published in our previous study.[22] Elemental composition analysis was carried out by

XPS (Axis Ultra instrument, Kratos, UK). We used GO (100 mg L^{-1}) as a control for this study. All the other chemicals were obtained from Sigma-Aldrich (St Louis, MO, USA).

Strain preparation

The information on the used nematode strains is given in Table S4.† Nematodes were maintained on nematode growth medium (NGM) plates seeded with *Escherichia coli* OP50 at 20 °C as described.[11] Age synchronous populations of L1-larvae were obtained as described previously.[39]

Exposure

Previous studies have suggested that L1-larvae may be more sensitive than L4-larvae or young adults to toxicants,[40,41] and the prolonged exposure or chronic exposure assay system of *C. elegans* can be used to assess the toxicity of ENMs at the predicted environmentally relevant concentrations.[15,42,43] Prolonged exposure to G-COOH or GO in K-medium (32 mmol L^{-1} KCl, 51 mmol L^{-1} NaCl) from L1-larvae to adult day-1 or chronic exposure to G-COOH or GO in K-medium from L1-larvae to adult day-10 was performed in 12-well sterile tissue culture plates at 20 °C in the presence of food (OP50). To assess the possible adverse effects of G-COOH or GO on the progeny of exposed nematodes, eggs were obtained from animals exposed to G-COOH or GO by treating with the bleaching mixture, and then transferred to a new NGM plate without addition of G-COOH or GO.

Distribution and translocation of G-COOH in nematodes

To investigate the translocation and distribution of G-COOH in nematodes, Rho B was loaded on G-COOH by mixing a Rho B solution (1 mg mL^{-1}, 0.3 mL) with an aqueous suspension of G-COOH (0.1 mg mL^{-1}, 5 mL) with the aid of shaking overnight basically as described for other carbon ENMs.[21,23,44] Unbound Rho B was removed by dialysis against distilled water over 72 h. The resulting G-COOH/Rho B was stored at 4 °C. The examined nematodes were incubated with G-COOH/Rho B (100 mg L^{-1}) for 3 h, and washed with M9 buffer three times. Rho B staining was used as the control. Nematodes were then observed under a laser scanning confocal microscope (Leica, TCS SP2, Bensheim, Germany). Graphene materials may be labeled by Rho B through p–p stacking, hydrophobic, and hydrogen-bonding interactions.[45]

Development, reproduction and locomotion behavior assays

The methods were performed as described previously.[16,46] Growth was assessed by the body length, which was determined by measuring the flat surface area of nematodes using Image-Pro® Express software. Thirty nematodes were performed per treatment. To assay the brood size, the number of offsprings at all stages beyond the egg was counted. Twenty nematodes were examined per treatment. Locomotion behavior was evaluated by the endpoints of head thrash and body bend. The examined nematodes were washed with K medium, and transferred into a microtiter well containing 60 μL of K medium on the top of agar. A head thrash was defined as a change in the direction of bending at the mid body. A body bend was counted as a change in the direction of the part of the nematodes corresponding to the posterior bulb of the pharynx along the *y* axis, assuming that the nematode was traveling along the *x* axis. Twenty nematodes were examined per treatment. Three replicates were performed.

Lifespan assay

Lifespan assay was performed basically as described.[47,48] In this test, hermaphrodites were transferred daily for the first 4 days of adulthood. Nematodes were checked every 2 days and would be scored as dead when they did not move even after repeated taps with a pick. Forty nematodes were examined per treatment. For lifespan, graphs are representative of at least three trials.

Intestinal ROS production

The method was performed as described previously.[49] To examine the ROS production, nematodes were transferred to 1 μmol L^{-1} 5′,6′-chloromethyl-2′,7′dichlorodihydrofluorescein diacetate (CM-H_2DCFDA; Molecular Probes) in 12-well sterile tissue culture plates to incubate for 3 h at 20 °C. CM-H_2DCFDA can specially detect the presence of various intracellular produced ROS species. Nematodes were mounted on 2% agar pads for examination with a laser scanning confocal microscope (Leica, TCS SP2, Bensheim, Germany) at 488 nm excitation wavelength and 510 nm emission filter. Semiquantified ROS was expressed as relative fluorescence units (RFU). Fifty nematodes were examined per treatment. Three replicates were performed.

Nile Red staining

The methods were performed as described previously.[21] Nile Red (Molecular Probes, Eugene, OR) was dissolved in acetone to produce a 0.5 mg mL^{-1} stock solution and stored at 4 °C. The stock solution was freshly diluted in 1 × PBS to 1 μg mL^{-1}, and 150 μL of the diluted solution was used for Nile Red staining. Twenty nematodes were examined per treatment. Three replicates were performed.

Defecation behavior analysis and fluorescence images of neurons controlling the defecation behavior

The method was performed as described previously.[30] To assay the mean defecation cycle length, individual animals were examined for a fixed number of cycles, and a cycle period was defined as the interval between initiations of two successive posterior body-wall muscle contraction steps. Thirty nematodes were examined per treatment. Three replicates were performed.

Fluorescence images of AVL and DVB neurons controlling the defecation behavior were captured with a Zeiss AxioCam MRm camera on a Zeiss Axioplan 2 Imaging System using the SlideBook software (Intelligent Imaging Innovations). Images were acquired with a Quantix CCD camera, and illumination was provided by using a 175 W xenon arc lamp and GFP filter sets. The relative sizes of fluorescent puncta for cell bodies of

AVL and DVB neurons were measured as the maximum radius for the assayed fluorescent puncta. The relative sizes of fluorescent puncta for cell bodies of neurons were examined in 20 nematodes. Three replicates were performed.

Electron microscopy

The method was performed as described previously.[30] Nematodes were fixed in 0.5% glutaraldehyde and 2% osmium tetroxide. The fixed nematodes were embedded in araldite resin following the infiltration series (30% araldite/acetone for 4 h, 70% araldite/acetone for 5 h, 90% araldite/acetone overnight, and pure araldite for 8 h). Serial sections were collected using an Ultracut E microtome. Images were obtained on a Hitachi H-7100 electron microscope using a Gatan slow scan digital camera.

Quantitative real-time polymerase chain reaction (qRT-PCR)

Total RNA was extracted using a RNeasy Mini Kit (Qiagen). Total RNA (~1 μg) was reverse-transcribed using a cDNA Synthesis Kit (Bio-Rad Laboratories). Quantitative reverse transcription PCR was run at the optimized annealing temperature of 58 °C. qRT-PCR and data analysis were performed using a LineGene 9600 Real-Time PCR system (Bioer Technology Co., Hangzhou, China). Data were considered to represent differentially expressed genes in qRT-PCR analysis if values for $2^{-\Delta\Delta CT}$ were up- or downregulated at least 2.0-fold compared to the control group in three independent experiments. Relative quantification of the targeted genes in comparison with the reference *tba-1* gene, encoding the tubulin, was determined. The final results were expressed as the relative expression ratio between the targeted gene and reference gene. The qRT-PCR results reflect the expression pattern of genes in the whole body of nematodes. The designed primers for the targeted genes and the reference *tba-1* gene are shown in Table S5.†

Statistical analysis

All data were presented as means ± standard error of the mean (S.E.M.). Graphs were generated using Microsoft Excel (Microsoft Corp., Redmond, WA). Statistical analysis was performed using SPSS 12.0 software (SPSS Inc., Chicago, USA). Differences between groups were determined using the analysis of variance (ANOVA). Probability levels of 0.05 and 0.01 were considered statistically significant.

Acknowledgements

Strains used in this study were provided by the *Caenorhabditis* Genetics Center (funded by the NIH National Center for Research Resource, USA). This work was supported by the grants from the National Basic Research Program of China (no. 2011CB33404), the National Natural Science Foundation of China (no. 81172698), the Jiangsu Province Ordinary University Graduate Research and Innovation Program (no. CXZZ13_0136), the Southeast University Outstanding Doctoral Foundation, and Fundamental Research Funds for the Central Universities.

References

1 L. Feng and Z. Liu, *Nanomedicine*, 2011, **6**, 317–324.
2 Y. Zhang, S. F. Ali, E. Dervishi, Y. Xu, Z. Li, D. Casciano and A. S. Biris, *ACS Nano*, 2010, **4**, 3181–3186.
3 K. Wang, J. Ruan, H. Song, J. Zhang, Y. Wo, S. Guo and D. Cui, *Nanoscale Res. Lett.*, 2011, **6**, 8.
4 A. Sasidharan, L. S. Panchakarla, P. Chandran, D. Menon, S. Nair, C. N. R. Rao and M. Koyakutty, *Nanoscale*, 2011, **3**, 2461–2464.
5 Y.-P. Li, Q.-L. Wu, Y.-L. Zhao, Y.-F. Bai, P.-S. Chen, T. Xia and D.-Y. Wang, *ACS Nano*, 2014, **8**, 2100–2110.
6 T. Lammel, P. Boisseaux, M. Fernandez-Cruz and J. M. Navas, *Part. Fibre Toxicol.*, 2013, **10**, 27.
7 H. Shen, L. Zhang, M. Liu and Z. Zhang, *Theranostics*, 2012, **2**, 283–294.
8 B. Liang, L. Fang, G. Yang, Y. Hu, X. Guo and X. Ye, *Biosens. Bioelectron.*, 2013, **43**, 131–136.
9 Q. Zhu, Y. Chai, R. Yuan, Y. Zhuo, J. Han and N. Liao, *Biosens. Bioelectron.*, 2013, **43**, 440–445.
10 A. Bonanni, C. K. Chua and M. Pumera, *Chemistry*, 2014, **20**, 217–222.
11 S. Brenner, *Genetics*, 1974, **77**, 71–94.
12 M. C. K. Leung, P. L. Williams, A. Benedetto, C. Au, K. J. Helmke, M. Aschner and J. N. Meyer, *Toxicol. Sci.*, 2008, **106**, 5–28.
13 J. Roh, S. J. Sim, J. Yi, K. Park, K. H. Chung, D. Ryu and J. Choi, *Environ. Sci. Technol.*, 2009, **43**, 3933–3940.
14 Y.-L. Zhao and D.-Y. Wang, *Oxid. Med. Cell. Longevity*, 2012, **2012**, 564093.
15 Y.-L. Zhao, Q.-L. Wu, Y.-P. Li and D.-Y. Wang, *RSC Adv.*, 2013, **3**, 5741–5757.
16 Q. Rui, Y.-L. Zhao, Q.-L. Wu, M. Tang and D.-Y. Wang, *Chemosphere*, 2013, **93**, 2289–2296.
17 N. Mohan, C. Chen, H. Hsieh, Y. Wu and H. Chang, *Nano Lett.*, 2010, **10**, 3692–3699.
18 Y. J. Cha, J. Lee and S. S. Choi, *Chemosphere*, 2012, **87**, 49–54.
19 P. H. Chen, K. M. Hsiao and C. C. Chou, *Biomaterials*, 2013, **34**, 5661–5669.
20 Q.-L. Wu, Y.-L. Zhao, G. Zhao and D.-Y. Wang, *Nanomedicine*, 2014, **10**, 1401–1410.
21 A. Nouara, Q.-L. Wu, Y.-X. Li, M. Tang, H.-F. Wang, Y.-L. Zhao and D.-Y. Wang, *Nanoscale*, 2013, **5**, 6088–6096.
22 Q.-L. Wu, L. Yin, X. Li, M. Tang, T. Zhang and D.-Y. Wang, *Nanoscale*, 2013, **5**, 9934–9943.
23 Q.-L. Wu, Y.-X. Li, Y.-P. Li, Y.-L. Zhao, L. Ge, H.-F. Wang and D.-Y. Wang, *Nanoscale*, 2013, **5**, 11166–11178.
24 Y.-L. Zhao, Q.-L. Wu, Y.-P. Li, A. Nouara, R.-H. Jia and D.-Y. Wang, *Nanoscale*, 2014, **6**, 4275–4284.
25 Q.-L. Wu, Y.-L. Zhao, J.-P. Fang and D.-Y. Wang, *Nanoscale*, 2014, **6**, 5894–5906.

26 Q.-L. Wu, Y.-L. Zhao, Y.-P. Li and D.-Y. Wang, *Nanoscale*, 2014, **6**, 11204–11212.
27 E. Zanni, G. De Bellis, M. P. Bracciale, A. Broggi, M. L. Santarelli, M. S. Sarto, C. Palleschi and D. Uccelletti, *Nano Lett.*, 2012, **12**, 2740–2744.
28 W. Zhang, C. Wang, Z. Li, Z. Lu, Y. Li, J. Yin, Y. Zhou, X. Gao, Y. Fang, G. Nie and Y. Zhao, *Adv. Mater.*, 2012, **24**, 5391–5397.
29 J. D. McGhee, *WormBook*, 2007, DOI: 10.1895/wormbook.1.133.1.
30 Y.-L. Zhao, Q.-L. Wu, M. Tang and D.-Y. Wang, *Nanomedicine*, 2014, **10**, 89–98.
31 S. Bhattacharjee, L. H. J. de Haan, N. M. Evers, X. Jiang, A. T. M. Marcelis, H. Zuilhof, I. M. Rietjens and G. M. Alink, *Part. Fibre Toxicol.*, 2010, **7**, 25.
32 S. Bhattacharjee, D. Ershov, K. Fytianos, J. van der Gucht, G. M. Alink, I. M. C. M. Rietjens, T. M. M. Antonius and H. Zuihof, *Part. Fibre Toxicol.*, 2012, **9**, 11.
33 A. Pluskota, E. Horzowski, O. Bossinger and A. von Mikecz, *PLoS One*, 2009, **4**, e6622.
34 J. Chen, C. Guo, M. Wang, L. Huang, L. Wang, C. Mi, J. Li, X. Fang, C. Mao and S. Xu, *J. Mater. Chem.*, 2011, **21**, 2632.
35 L. A. del Río, L. M. Sandalio, J. M. Palma, P. Bueno and F. J. Corpas, *Free Radicals Biol. Med.*, 1992, **13**, 557–580.
36 C. Settembre, A. Fraldi, D. L. Medina and A. Ballabio, *Nat. Rev. Mol. Cell Biol.*, 2013, **14**, 283–296.
37 S. Bhattacharjee, D. Ershov, M. A. Islam, A. M. Kampfer, K. A. Maslowska, J. van der Gucht, G. M. Alink, A. T. M. Marcelis, H. Zuihof and I. M. C. M. Rietjens, *RSC Adv.*, 2014, **4**, 19321–19330.
38 N. I. Kovtyukhova, P. J. Olivier, B. R. Martin, T. E. Mallouk, S. A. Chizhik, E. V. Buzaneva and A. D. Gorchinskiy, *Chem. Mater.*, 1999, **11**, 771–778.
39 S. G. Donkin and D. B. Dusenbery, *Arch. Environ. Contam. Toxicol.*, 1993, **25**, 145–151.
40 X.-J. Xing and D.-Y. Wang, *Bull. Environ. Contam. Toxicol.*, 2009, **83**, 530–536.
41 S. Wu, J.-H. Lu, Q. Rui, S.-H. Yu, T. Cai and D.-Y. Wang, *Environ. Toxicol. Pharmacol.*, 2011, **31**, 179–188.
42 Y.-X. Li, W. Wang, Q.-L. Wu, Y.-P. Li, M. Tang, B.-P. Ye and D.-Y. Wang, *PLoS One*, 2012, **7**, e44688.
43 Q.-L. Wu, W. Wang, Y.-X. Li, Y.-P. Li, B.-P. Ye, M. Tang and D.-Y. Wang, *J. Hazard. Mater.*, 2012, **243**, 161–168.
44 Q.-L. Wu, A. Nouara, Y.-P. Li, M. Zhang, W. Wang, M. Tang, B.-P. Ye, J.-D. Ding and D.-Y. Wang, *Chemosphere*, 2013, **90**, 1123–1131.
45 L. Zhang, J. Xia, Q. Zhao, L. Liu and Z. Zhang, *Small*, 2010, **6**, 537–544.
46 Y.-X. Li, S.-H. Yu, Q.-L. Wu, M. Tang and D.-Y. Wang, *Nanotoxicology*, 2013, **7**, 1004–1013.
47 L.-L. Shen, Y.-O. Hu, T. Cai, X.-F. Lin and D.-Y. Wang, *Mech. Ageing Dev.*, 2010, **131**, 732–738.
48 D.-Y. Wang, M. Cao, J. Dinh and Y.-Q. Dong, *Method Mol. Biol.*, 2013, **1048**, 65–75.
49 W.-M. Zhang, T. Lv, M. Li, Q.-L. Wu, L.-S. Yang, H. Liu, D.-F. Sun, L.-M. Sun, Z.-H. Zhuang and D.-Y. Wang, *PLoS One*, 2013, **8**, e74553.